

See discussions, stats, and author profiles for this publication at: <https://www.researchgate.net/publication/41120927>

# Probing Pore Connectivity in Random Porous Materials by Scanning Freezing and Melting Experiments

ARTICLE *in* LANGMUIR · MAY 2010

Impact Factor: 4.46 · DOI: 10.1021/la904062h · Source: PubMed

---

CITATIONS

20

---

READS

18

3 AUTHORS, INCLUDING:



**Daria Kondrashova**

University of Leipzig

8 PUBLICATIONS 33 CITATIONS

SEE PROFILE



**Rustem Valiullin**

University of Leipzig

137 PUBLICATIONS 1,673 CITATIONS

SEE PROFILE

## Probing Pore Connectivity in Random Porous Materials by Scanning Freezing and Melting Experiments

D. Kondrashova, C. Reichenbach, and R. Valiullin\*

Department of Interface Physics, University of Leipzig, Linnéstr. 5, D-04103 Leipzig, Germany

Received October 26, 2009. Revised Manuscript Received December 23, 2009

Freezing and melting behavior of nitrobenzene confined to pores of Vycor porous glass with random pore structure has been studied by means of nuclear magnetic resonance cryoporometry. The two transitions are found to reveal a broad hysteresis. To get deeper insight into the mechanisms leading to this phenomenon, scanning experiments exploiting temperature reversal upon incomplete freezing or melting have been performed. In this way, it was found that different cooling and warming histories result in different solid–liquid configurations within the pore system. Further evolution of the thus-attained configurations with changing temperature unveiled important information about the transition paths. In particular, these experiments indicated the occurrence of a pronounced pore blocking for freezing, resulting in freezing transitions via invasion percolation. The melting, on the other hand, is found to occur homogeneously over the whole pore network.

### Introduction

Fluids confined to mesopores often exhibit a rich variety of phenomena not typical for bulk substances.<sup>1</sup> Among them, hysteretic melting–freezing phase transitions have attracted particular attention and have been thoroughly studied.<sup>2–16</sup> Despite long history and diversity of related studies, some aspects accompanying these transitions are still not fully understood. Discovery of mesoporous materials with uniform, channel-like pores, such as MCM-41<sup>17</sup> or SBA-15,<sup>18</sup> has greatly promoted fundamental understanding of confinement effects upon melting and freezing transitions. Because of their simple pore structure, these materials provided unique option to avoid complicated network effects and to focus solely on how the confinement size affects the fluid phase

state. In particular, they helped to verify the applicability of the Gibbs–Thomson equation, which relates the shifts of the transition temperatures to the pore size. Thus, it was shown that this equation properly reproduces the melting transition in pores. Therefore, the formation of hysteresis has been associated with metastable freezing.<sup>5,9,19–21</sup>

Structural disorder may substantially affect the mechanisms leading to hysteresis formation in mesopores. As a representative example, the recently emerged ordered mesoporous materials with ink-bottle pore geometry (KIT-5, mesoporous silicon) have allowed to experimentally confirm the relevance of pore blocking on the freezing transition.<sup>13,14</sup> In addition, it was shown that for sufficiently narrow necks (strong pore blocking) the liquid in the bottle pores may freeze via the mechanism of homogeneous nucleation.<sup>14</sup> For materials with disordered pore structure, which may be considered as pore networks with a certain distribution of pore sizes and pore geometries, these features may lead to very complex patterns of crystal growth within pores. Although being argued for a long time to be relevant for the freezing of fluids in disordered porous materials,<sup>22</sup> it has only recently become possible to be experimentally demonstrated it by using mesoporous silicon with one-dimensional, tubular pores with an intentionally created statistical distribution of the pore diameters using combined diffusion and cryoporometry measurements.<sup>23</sup>

In random materials with three-dimensional pore networks, such as Vycor porous glass, the crystal growth process is expected to be even more complicated and might, in principle, be described in terms of invasion percolation.<sup>24</sup> Indeed, such a process, namely the formation of a fractal-like network, has been found to occur during a related physical process of desorption from Vycor

\*To whom correspondence should be addressed. E-mail: valiullin@uni-leipzig.de.

(1) Gelb, L. D.; Gubbins, K. E.; Radhakrishnan, R.; Sliwinski-Bartkowiak, M. *Rep. Prog. Phys.* **1999**, *62*, 1573–1659.

(2) Molz, E.; Wong, A. P. Y.; Chan, M. H. W.; Beamish, J. R. *Phys. Rev. B* **1993**, *48*, 5741–5750.

(3) Unruh, K. M.; Huber, T. E.; Huber, C. A. *Phys. Rev. B* **1993**, *48*, 9021–9027.

(4) Sliwinski-Bartkowiak, M.; Gras, J.; Sikorski, R.; Radhakrishnan, R.; Gelb, L.; Gubbins, K. E. *Langmuir* **1999**, *15*, 6060–6069.

(5) Morishige, K.; Kawano, K. *J. Chem. Phys.* **1999**, *110*, 4867–4872.

(6) Faivre, C.; Bellet, D.; Dolino, G. *Eur. Phys. J. B* **1999**, *7*, 19–36.

(7) Christenson, H. K. *J. Phys.: Condens. Matter* **2001**, *13*, R95–R133.

(8) Wallacher, D.; Knorr, K. *Phys. Rev. B* **2001**, *63*, 104202.

(9) Schreiber, A.; Ketelsen, I.; Findenegg, G. H. *Phys. Chem. Chem. Phys.* **2001**, *3*, 1185–1195.

(10) Denoyel, R.; Pellenq, R. J. M. *Langmuir* **2002**, *18*, 2710–2716.

(11) Soprunyuk, V. P.; Wallacher, D.; Huber, P.; Knorr, K.; Kityk, A. V. *Phys. Rev. B* **2003**, *67*, 144105.

(12) Petrov, O.; Furó, I. *Phys. Rev. E* **2006**, *73*, 011608.

(13) Morishige, K.; Yasunaga, H.; Denoyel, R.; Wernert, V. *J. Phys. Chem. C* **2007**, *111*, 9488–9495.

(14) Khokhlov, A.; Valiullin, R.; Kärger, J.; Steinbach, F.; Feldhoff, A. *New J. Phys.* **2007**, *9*, 272.

(15) Schaefer, C.; Hofmann, T.; Wallacher, D.; Huber, P.; Knorr, K. *Phys. Rev. Lett.* **2008**, *100*, 175701–4.

(16) Knorr, K.; Huber, P.; Wallacher, D. *Z. Phys. Chem. (Munich)* **2008**, *222*, 257–285.

(17) Beck, J. S.; Vartuli, J. C.; Roth, W. J.; Leonowicz, M. E.; Kresge, C. T.; Schmitt, K. D.; Chu, C. T. W.; Olson, D. H.; Sheppard, E. W.; McCullen, S. B.; Higgins, J. B.; Schlenker, J. L. *J. Am. Chem. Soc.* **1992**, *114*, 10834–10843.

(18) Zhao, D.; Feng, J.; Huo, Q.; Melosh, N.; Fredrickson, G. H.; Chmelka, B. F.; Stucky, G. D. *Science* **1998**, *279*, 548–552.

(19) Morishige, K.; Iwasaki, H. *Langmuir* **2003**, *19*, 2808–2811.

(20) Jahnert, S.; Chavez, F. V.; Schaumann, G. E.; Schreiber, A.; Schonhoff, M.; Findenegg, G. H. *Phys. Chem. Chem. Phys.* **2008**, *10*, 6039–6051.

(21) Findenegg, G. H.; Jahnert, S.; Akcakayiran, D.; Schreiber, A. *ChemPhysChem* **2008**, *9*, 2651–2659.

(22) Swainson, I. P.; Schulson, E. M. *Cem. Concr. Res.* **2001**, *31*, 1821–1830.

(23) Dvoyashkin, M.; Khokhlov, A.; Valiullin, R.; Kärger, J. *J. Chem. Phys.* **2008**, *129*, 154702–6.

(24) Bunde, A.; Shlomo, H. Percolation I. In *Fractals and Disordered Systems*, 2nd ed.; Bunde, A., Shlomo, H., Eds.; Springer-Verlag: Berlin, 1996.

porous glass.<sup>25–27</sup> Recently, Perkins et al. have experimentally demonstrated that percolation effects are also observed during freezing.<sup>28</sup> Combining cryoporometry and diffusometry and using a mesoporous sol–gel silica material with highly disordered pore structure, they have been able to isolate the pore-blocking effect from other material properties, determining the freezing behavior. Further analysis has been performed using percolation theory.

As we have noted, in addition to pore-size distribution, network effects due to interconnections between different pores may strongly affect the shape of the hysteresis. In practice, it is not straightforward to separate them from each other based on solely hysteresis measurements. In addition, quantitative analysis of the hysteresis is partly prohibited due to the lack of consistency existing in the literature concerning which of the transitions, freezing or melting, is associated with the equilibrium transition in disordered materials.<sup>8,10,12,29</sup> In gas sorption studies, where the same type of problems do exist, some enlightening information has been obtained by so-called scanning experiments.<sup>30–35</sup> They imply reversals into the desorption branch before complete filling and into the adsorption branch before complete emptying of the mesopores. In this way, for example, it has been shown that network mechanisms are predominant for sorption hysteresis of xenon in Vycor porous glass.<sup>36</sup>

Because of many similarities between the processes of adsorption/desorption and melting/freezing under confinement,<sup>37</sup> scanning freezing and melting experiments are as well expected to provide further insight into the mechanisms of the hysteresis formation in random porous materials. Notably, this type of experiment has not been systematically performed.<sup>2</sup> Rather, an alternative approach has often been undertaken where freezing and melting behavior of fluids in partially filled pores has been investigated.<sup>8,9,11,15,19</sup> In this work, we complement these studies by measuring melting and freezing scanning behavior of a fluid in random Vycor porous glass using NMR cryoporometry,<sup>38–40</sup> which directly probes the relative compositions of the frozen and liquid phases at different temperatures.

## Experimental Section

All experiments in the present study have been performed using Vycor porous glass<sup>41</sup> possessing a random pore structure, a

relatively narrow pore size distribution centered at a pore diameter of about 6 nm, and a porosity of about 27%. More detailed information about its structural characteristics may be found elsewhere.<sup>42,43</sup> The porous glass was applied as a monolithic rodlike body with a diameter of 6 mm and a length of 12 mm. Prior to saturation by a liquid under study, it was placed in a glass tube, cleaned by boiling in H<sub>2</sub>O<sub>2</sub>, and outgassed. Saturation was accomplished by external impregnation under vacuum by an amount of liquid sufficient to provide complete filling of the mesopores by the liquid and to completely cover the Vycor particle by the excess fluid. Nitrobenzene was used as a probe liquid, which is found to be a suitable liquid for NMR cryoporometry experiments.<sup>14</sup>

<sup>1</sup>H NMR cryoporometry experiments<sup>38–40</sup> have been performed using a spectrometer operating at 400 MHz for protons. The Hahn-echo pulse sequence with an interpulse delay of  $\tau = 3$  ms was used. Since frozen nitrobenzene has very short transverse relaxation times  $T_2$  of the order of tens of microseconds, i.e., much smaller than the interpulse delay  $\tau$ , it does not contribute to the spin–echo signal. So that the measured intensity  $I$  is proportional to the number of protons (hence, molecules) in the liquid phase. The thus-compiled function  $I(T)$ , namely the relative volume of the liquid phase in the pores, will be analyzed and will be further referred to as the freezing (measured on the cooling branch) and melting (measured on the heating branch) curve. It has to be noted that, by changing the temperature  $I(T)$ , varies not only due to freezing or melting but also due to the Curie effect (i.e., the proportionality between nuclear magnetization and the inverse temperature) and the temperature dependence of  $T_2$  in the liquid phase. The results, which will be shown in the paper, were corrected for both effects. The former was accounted for by multiplying the measured function  $I(T)$  by  $T$  and the latter by directly measuring  $T_2$  of the supercooled liquid in the pores as a function of  $T$  and making the corresponding normalization. During the experiments, the temperature stability was kept to  $\approx 0.2$  °C. Upon changing the temperature, 10 min time was given for the equilibration before measurements. It was ensured that after this period of time only minor changes of the signal intensity were observed.

## Results and Discussion

**Boundary Hysteresis Loop.** Figure 1 shows the freezing and melting curves of nitrobenzene in Vycor porous glass. The measurement procedure was as follows. First, the sample was cooled down to about  $-70$  °C. At this temperature both the excess bulk and nitrobenzene in the pores freeze completely; i.e., almost no spin–echo signal is observed. Although the existence of the nonfrozen surface layers adjacent to the pore walls is known from previous NMR studies,<sup>44–47</sup> liquids in such layers typically have relatively short transverse relaxation times as compared to  $\tau = 3$  ms used in this work. Hence, they do have only a minor contribution to the measured signal and, therefore, will be excluded from further consideration. Thereafter, temperature was increased by a certain degree (e.g., 1 °C). After 10 min, given for the equilibration, the spin–echo signal intensity  $I(T)$  was measured. This procedure was repeated until about 0 °C, yielding the melting curve. At this temperature, the direction of the temperature change was inverted and the freezing curve was measured in the same manner. Note that the bulk melting temperature of

- (25) Li, J.-C.; Ross, D. K.; Benham, M. J. *J. Appl. Crystallogr.* **1991**, *24*, 794–802.
- (26) Li, J. C.; Ross, D. K.; Howe, L. D.; Stefanopoulos, K. L.; Fairclough, J. P. A.; Heenan, R.; Ibel, K. *Phys. Rev. B* **1994**, *49*, 5911–5917.
- (27) Page, J. H.; Liu, J.; Abeles, B.; Herbolzheimer, E.; Deckman, H. W.; Weitz, D. A. *Phys. Rev. E* **1995**, *52*, 2763–2777.
- (28) Perkins, E. L.; Lowe, J. P.; Edler, K. J.; Tanko, N.; Rigby, S. P. *Chem. Eng. Sci.* **2008**, *63*, 1929–1940.
- (29) Warnock, J.; Awschalom, D. D.; Shafer, M. W. *Phys. Rev. Lett.* **1986**, *57*, 1753 LP–1756.
- (30) Everett, D. H. Adsorption hysteresis. In *The Solid-Gas Interface*; Alison Flood, E., Ed.; Marcel Dekker: New York, 1967; pp 1055–1113.
- (31) Kierlik, E.; Monson, P. A.; Rosinberg, M. L.; Tarjus, G. *J. Phys.: Condens. Matter* **2002**, *14*, 9295–9315.
- (32) Esparza, J. M.; Ojeda, M. L.; Campero, A.; Dominguez, A.; Kornhauser, I.; Rojas, F.; Vidales, A. M.; Lopez, R. H.; Zgrablich, G. *Colloids Surf., A* **2004**, *241*, 35–45.
- (33) Soos, M.; Rajniak, P.; Stepanek, F. *Colloids Surf., A* **2007**, *300*, 191–203.
- (34) Grosman, A.; Ortega, C. *Langmuir* **2008**, *24*, 3977–3986.
- (35) Naumov, S.; Valiullin, R.; Monson, P. A.; Kärger, J. *Langmuir* **2008**, *24*, 6429–6432.
- (36) Ball, P. C.; Evans, R. *Langmuir* **1989**, *5*, 714–723.
- (37) Beurroies, I.; Denoyel, R.; Llewellyn, P.; Rouquerol, J. *Thermochim. Acta* **2004**, *421*, 11–18.
- (38) Strange, J. H.; Rahman, M.; Smith, E. G. *Phys. Rev. Lett.* **1993**, *71*, 3589–3591.
- (39) Mitchell, J.; Webber, J. B. W.; Strange, J. *Phys. Rep.* **2008**, *461*, 1–36.
- (40) Petrov, O. V.; Fúró, I. *Prog. Nucl. Magn. Reson. Spectrosc.* **2009**, *54*, 97–122.
- (41) Elmer, T. H. Porous and reconstructed glasses. In *Engineered Materials Handbook*; ASM: Materials Park, OH, 1992; Vol. 4, pp 427–432.

- (42) Wiltzius, P.; Bates, F. S.; Dierker, S. B.; Wignall, G. D. *Phys. Rev. A* **1987**, *36*, 2991–2994.
- (43) Pellenq, R. J. M.; Rousseau, B.; Levitz, P. E. *Phys. Chem. Chem. Phys.* **2001**, *3*, 1207–1212.
- (44) Overloop, K.; Vangerven, L. J. *Magn. Reson. A* **1993**, *101*, 179–187.
- (45) Stapf, S.; Kimmich, R. *J. Chem. Phys.* **1995**, *103*, 2247–2250.
- (46) Valiullin, R.; Furo, I. *J. Chem. Phys.* **2002**, *117*, 2307–2316.
- (47) Petrov, O.; Vargas-Florencia, D.; Furo, I. *J. Phys. Chem. B* **2007**, *111*, 1574–1581.

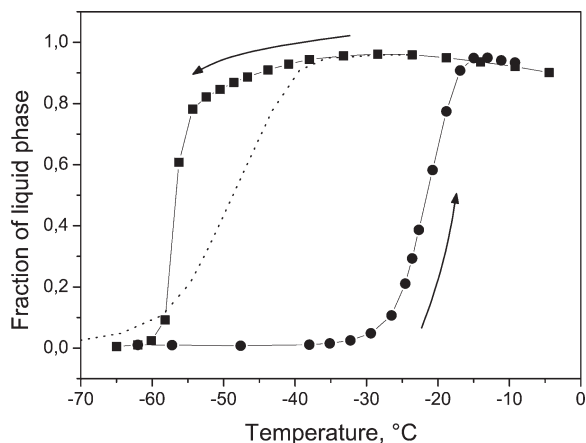


**Figure 1.** Freezing (squares) and melting (circles) curves of nitrobenzene in Vycor porous glass, representing the relative fractions of the liquid phase in the pores measured upon cooling and heating, respectively. The solid lines are shown to guide the eye. The dotted line shows the expected freezing curve, calculated assuming that Vycor glass is composed of independent cylindrical pores and the transitions in them occur independently at equilibrium with the bulk phase (see text for more details).

nitrobenzene is  $T_0 \approx 5.6$  °C. Thus, it is in the frozen state throughout all experiments and, due to its short nuclear transverse relaxation times, does not contribute, therefore, to the measured signal.

The experimental results in Figure 1 unveil two transitions occurring in sufficiently distinct temperature ranges, leading to a pronounced hysteresis between freezing and melting. The shape of hysteresis was found to be extremely reproducible; i.e., the results of different experiments with one and the same sample coincided within the experimental error. As has already been discussed in the literature, three different mechanisms may contribute to the formation of the hysteresis (see, e.g., ref 12 where they were summarized): (i) delayed homogeneous nucleation in pores upon cooling, (ii) pore-blocking mechanism, and (iii) the occurrence of metastable states separated from stable ones by large barriers in the free energy. To estimate their relevance for the system under study, we first shortly outline some thermodynamical aspects of solid–liquid phase equilibria in simplified pore geometries.

Consider an ideal cylindrical pore with a diameter of  $d$  filled with a liquid and having direct contact to the bulk frozen phase at both pore ends (Figure 2a,b). Note that this schematic captures the conditions under which our experiments have been performed. The difference in the free energy  $\Delta F_{sl}(T)$  (per unit length) between the two states (a) and (b) in Figure 2, namely the pore containing the solid core with a diameter of  $d_c$  and the pore filled by the liquid, respectively, is given by

$$\Delta F_{sl}(T) = -\frac{L(T_0 - T)\pi d_c^2}{vT_0 4} + \gamma_{sl}\pi d_c \quad (1)$$

Here,  $L$  is the heat of fusion,  $T$  is the temperature,  $T_0$  is the bulk melting temperature,  $v$  is the molar volume, and  $\gamma_{sl}$  is the surface energy. In eq 1, we did not include a term taking account of the interaction of the solid–liquid and liquid–pore wall interfaces (see, e.g., ref 47 for more detail and references therein). In the context of this work, the explicit consideration of this interaction will have an only quantitative but no qualitative effect and, therefore, will not be considered.

As has been mentioned in the Introduction, there is currently a controversy to associate the equilibrium transition (occurring

when the condition  $\Delta F_{sl} = 0$  is fulfilled) with the freezing or with the melting one. For further discussion, we will use a phenomenological model suggested by Denoyel and Pellenq.<sup>10</sup> The reason why we follow this model is that it provides the basis to quantify both transition temperatures. Within this model, it is assumed that freezing in pores occurs at equilibrium. The authors note that this is valid when overcoming of nucleation barriers, typical for homogeneous nucleation, is not a limiting step for freezing. It is further argued that it may be true if the cryoporometry experiments are performed in the presence of the excess liquid.<sup>12</sup> In this case, the direct contact of the intrapore fluid with the bulk frozen phase provides the initial nuclei of the solid phase at the pore openings. Under this assumption, using eq 1, the freezing temperature is evaluated to

$$T_{fr} = T_0 - \frac{4vT_0\gamma_{sl}}{Ld_c} = T_0 - \frac{2k}{d_c} \quad (2)$$

where we have defined  $k \equiv 2vT_0\gamma_{sl}/L$ . At this temperature, the solid front can penetrate into the pore throats and can advance further to fill the whole pore.

The model also quantitatively treats the melting transition. It is anticipated that with the frozen core, which fills the pore interior (Figure 2b), melting occurs by shrinking the solid core in radial direction. This requires overcoming the free energy barrier associated with the increase of the surface-to-volume ratio of the solid core upon reducing its size. Therefore, the melting temperature may be found using the condition  $\partial\Delta F_{sl}/\partial d_c = 0$ , i.e., finding a temperature at which the barrier in the free energy vanishes. This results in

$$T_m = T_0 - \frac{2vT_0\gamma_{sl}}{Ld_c} = T_0 - \frac{k}{d_c} \quad (3)$$

Because the parameter  $k \approx 125$  K nm for nitrobenzene, used in this study, is not independently known (its value was estimated from the melting point suppression of nitrobenzene in CPG porous glasses with different pore sizes using Gibbs–Thomson equation of type eq 2<sup>4,48</sup>), the predictions of eqs 2 and 3 cannot be directly compared to the experimental data to identify the equilibrium transition point. Therefore, we have combined these two equations to exclude  $k$ <sup>12</sup> and to relate the freezing and melting transition temperatures to each other. The thus-obtained relation, namely

$$T_{fr} - T_0 = 2(T_m - T_0) \quad (4)$$

may be used to, e.g., predict the freezing temperatures in an ideal cylindrical pore on the basis of the data on melting. Thus, assuming that the pore structure is composed of a system of independent cylindrical pores with a certain distribution of the pore sizes, the variation of the liquid fraction in the pores with decreasing temperature may easily be estimated on the basis of eq 4. Such an estimate is shown by the dotted line in Figure 1.

Comparison with the experimental data reveals that this model does not satisfactorily describe the experimental data for Vycor porous glass. The experimentally obtained transition occurs at lower temperatures and is more abrupt. However, it has to be noted that the onset of the transition temperature  $T_{tr}$  coincides with the prediction of eq 4 for the smallest pores. Therefore, the observed behavior might be associated with the occurrence of pore blocking, as schematically shown in Figure 2c: A bigger pore, surrounded by smaller necks, cannot freeze until the solid–liquid interface can pass through the necks. The occurrence of such a

(48) Valiullin, R.; Furo, I. *Phys. Rev. E* **2002**, *66*, 031508.



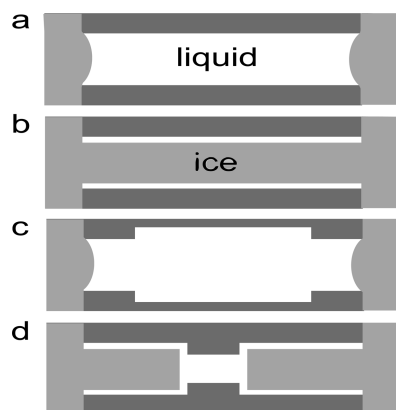


**Figure 2.** Schematic view of a cylindrical pore filled with the liquid phase (a) and with the frozen solid core (b), an ink-bottle pore (c), and a pore with a narrowing in the middle part (d). In all cases, the pore entrances are in immediate contact with the frozen phase.

freezing scenario in ink-bottle pores has recently been experimentally verified.<sup>13,14</sup> Note that freezing via homogeneous nucleation in the bigger pores may change this picture. However, the occurrence of homogeneous nucleation at these temperatures is expected only in sufficiently big pores. Indeed, these types of studies have been performed with mesoporous silicon with ink-bottle pores: The neck size (of about 6 nm) was comparable to the typical pore size in Vycor porous glass. With a diameter of the bottle pores of about 7.5 nm, the freezing mechanism via homogeneous nucleation was strongly suppressed and was found to be relevant for pores with a diameter of about 10 nm. Taking account of a relatively narrow pore size distribution in Vycor porous glass, we may render homogeneous nucleation in the material under study very improbable.

Considering only the boundary hysteresis loop, the following picture might be anticipated. Because of the preparation procedure, namely spinodal decomposition of a borosilicate glass, the pore structure of Vycor porous glass may be considered as a network of segments with varying pore sizes. Upon cooling, starting at about  $-40^{\circ}\text{C}$ , the solid phase can ingress into sufficiently big pores (satisfying the condition of eq 2 for this temperature) at the porous glass–bulk phase boundary. Upon further cooling, percolation clusters<sup>24</sup> may further grow along the favorable pathways. According to the experimental data, these clusters may occupy up to about 20% of the total pore volume. Starting at about  $-54^{\circ}\text{C}$ , the percolation threshold is presumably reached and percolating clusters spanning over the whole porous particle can be formed, leading to the complete freezing. Although this scenario reasonably explains the shape of the hysteresis loop, as we will see later, it does not capture the whole behavior. Here we also would mention that even if eq 4, combined with the pore-blocking mechanism, may be valid for the description of the hysteresis behavior, it does not prove or disprove the model behind eqs 2 and 3. Indeed, such a 2-fold difference in eq 4 may originate from other mechanisms of melting and freezing under confinements.

**Scanning Behavior.** Taking the point of view that freezing in uniform single ideal pores occurs at equilibrium, one may argue that closing one pore end should eliminate the hysteresis, similar to the situation discussed in the context of adsorption hysteresis.<sup>49</sup> Because of the existence of the nonfrozen surface layer, the frozen domain in a cylindrical pore will have contact to the liquid layer adjacent to the closed pore end. According to eq 1, at a

temperature just slightly above  $T_{\text{fr}}$  the liquid-filled pore has a lower free energy as compared to that with the frozen core. Therefore, reducing the size of the frozen domain in the axial direction by moving the solid–liquid interface toward the pore opening is thermodynamically favored. The same effect has to be expected if there exists a narrowing in the middle part of the pore (Figure 2d). At a certain temperature, the solid–liquid configuration shown in Figure 2d can be attained on heating. Further heating may lead to melting via moving the thus created solid–liquid interfaces in axial direction. In this way, it may be expected that metastable states associated with radial melting can be avoided. Notably, a similar phenomenon, the so-called advanced adsorption, has also been discussed with respect to liquid condensation in mesopores with nonuniform pore geometries.<sup>32,50</sup>

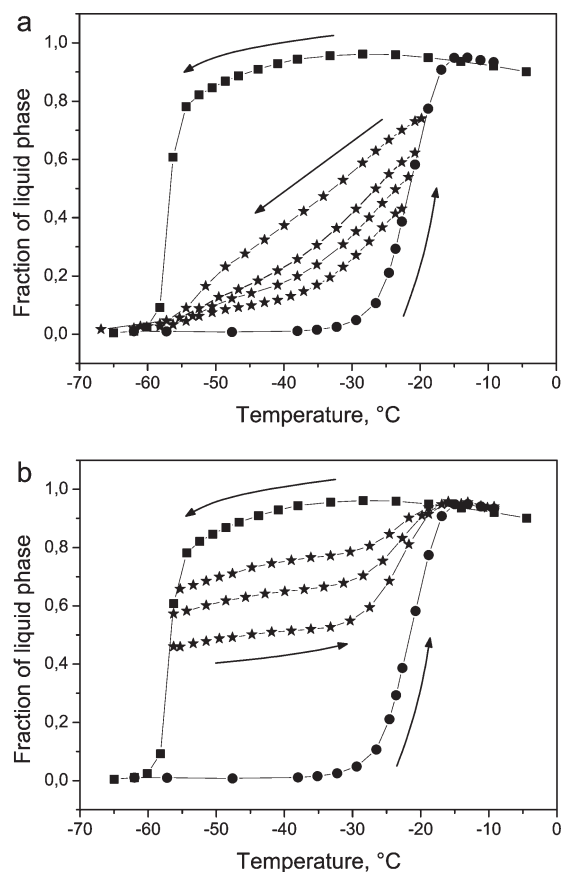
The relevance of this mechanism for melting may be assessed based on earlier experimental studies of the freezing and melting behavior in partially filled materials with uniform channel-like pores, like SBA-15 or MCM-41.<sup>9,19</sup> In these works, it has been found that the melting temperature is almost independent of the pore filling and coincides with that of the completely filled pores. This means that, irrespective of the existence of the intentionally created phase boundaries upon freezing of the separated liquid domains in the partially saturated channels, melting via shrinking of these domains in axial direction has not been observed. However, this type of experiment involves coexistence of three phases (gas, liquid, and solid), which may lead to temperature-dependent spatial phase redistributions. In fact, such a redistribution has been found to occur in partially filled Vycor porous glass.<sup>11</sup> In the present work, we have further addressed this issue by performing scanning experiments, which have earlier been widely used to study network effects on sorption behavior.<sup>30–35</sup>

Figure 3b shows the results of the melting scanning experiments. The measurement procedure was as follows. First, some part of the liquid in the pores was frozen upon cooling, leaving the other part of the pores filled with the liquid phase. Thereafter, the temperature was increased by some steps and the fraction of nitrobenzene in the liquid state was measured after a given equilibration time. The data obtained reveal two melting regimes. Initially, in the temperature range up to about  $-30^{\circ}\text{C}$ , melting of a minor part (of up to about 10% of the total pore volume) is observed. Starting from temperatures of about  $-30^{\circ}\text{C}$ , however, with further temperature increase the melting rate (with respect to temperature) increases. Notably, exactly in this temperature range melting upon warming of the system, initially being in the completely frozen state, is observed (the melting branch of the boundary hysteresis loop).

These experimental results allow making the following conclusions: (i) The hysteresis is not eliminated by the existence of the radial solid–liquid interfaces, i.e., preexisting nuclei of the capillary-condensed phase spanning over whole pore cross-section. (ii) Melting by moving the solid–liquid interface in the direction of the pore axis has a minor effect, at least for materials with random pore geometries. Note that if such a process would not exist at all, one then should observe a plateau-like behavior for the melting scanning curves immediately upon the temperature inversion. In fact, as a possible mechanism for the observed slight increase of the liquid fraction below  $-30^{\circ}\text{C}$ , one may anticipate, for example, the elimination of the dead ends (as exemplified in Figure 4). If it does occur, due to networked pore structure such a process will also eliminate radial solid–liquid interfaces, postponing the melting condition to the higher temperatures. However,

(49) Cohan, L. H. *J. Am. Chem. Soc.* **1938**, *60*, 433–435.

(50) Mayagoitia, V.; Rojas, F.; Kornhauser, I. *J. Chem. Soc., Faraday Trans. 1* **1985**, *81*, 2931–2940.



**Figure 3.** Freezing (a) and melting (b) scanning curves (stars) measured upon cooling, preceded by partial melting of frozen nitrobenzene in the pores, and upon heating, preceded by a partial freezing of the fluid, respectively. The squares and circles represent the main hysteresis loop (the same as in Figure 1).

we cannot exclude other processes, such as the rearrangement of the frozen domains, leading to the slight increase of the molten fraction at intermediate temperatures.

In a similar way, the freezing scanning experiments have also been performed. Figure 3a shows the freezing scanning curves obtained by inverting temperature at a point, where prior to cooling a certain fraction of the pores containing the frozen core has been attained by warming from the completely frozen state. Similar to the two regimes revealed by the melting scanning curves, two different regimes are also evident from the freezing scanning behavior. It is especially visible for the scanning curve which had been started with the initial 40% molten phase (the upper scanning curve in Figure 3a). It shows initial decrease of the freezing rate with decreasing temperature. However, at temperatures of about  $-50$  °C, the freezing process accelerates. This temperature closely coincides with the onset of the freezing in the pores obtained upon cooling the porous glass initially completely filled with the liquid phase.

Quite importantly, however, freezing is found to occur immediately upon the temperature reverse. A similar observation has earlier been also revealed from ultrasonic measurements.<sup>2</sup> If one considers freezing as a process taking place at equilibrium conditions, it is expected that the liquid even in the biggest pores will start to freeze at only about  $-40$  °C (the expected equilibrium freezing curve for a system of independent pores within the model by Denoyel and Pellenq is shown by the dotted line in Figure 1). In our case, freezing is already pronounced at  $-20$  °C (see, e.g., the upper scanning curve in Figure 3a). Thus, altogether, the results

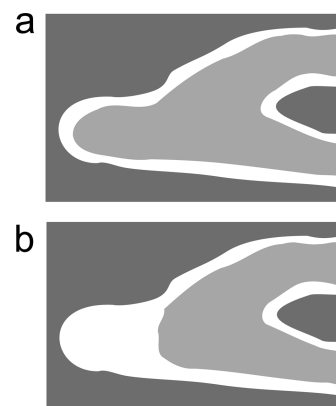


**Figure 4.** Schematic representation of a pore section with a dead end with the frozen (a) core and molten (b) core.

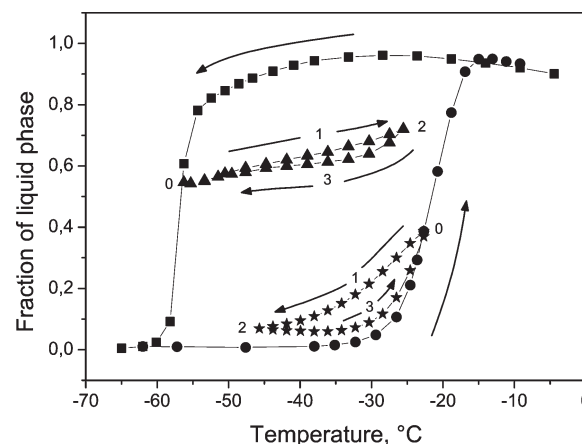


**Figure 5.** Freezing (triangles) and melting (stars) scanning loops measured during incomplete freezing and melting cycles. The numbers in the figure indicate the direction (0123) of temperature change starting from the initial point (0). The squares and circles show the boundary hysteresis loop (the same as in Figure 1).

of the melting and, especially, the freezing scanning experiments seem to not support the model of equilibrium freezing and may be more naturally explained assuming that the equilibrium temperature is located at higher temperatures.

To get more information, it was instructive to perform additional scanning experiments designed to have more complex histories of the cooling and warming branches. In the first experiment (triangles in Figure 5), the melting scanning curve had been stopped at an intermediate temperature before all frozen phase in the pores melts. Thus, some part of the pores still contained the frozen phase. Thereafter, the freezing process was quantified upon temperature decrease. In the second one (stars in Figure 5), the partial freezing scanning curve was followed by the melting one. It is interesting to note that in the both experiments the loops terminate at the initial points, exhibiting the so-called return-point memory. In addition, they cannot be superimposed on top of each other just by a shift along the vertical axis, which is often referred to as the lack of congruence.<sup>30,31,34</sup> These two properties of the scanning loops have important meanings. The former points out that the system evolution, the free energy landscape of which is very complex and very rugged, is predominantly driven by the change of the external parameters, namely temperature. The latter is considered to be a property of the interconnected systems.

Furthermore, the scanning loops bring about an additional evidence for strong pore-blocking, and, therefore, freezing via invasion percolation. Let us compare two freezing curves: (i) the upper one in Figure 3a and (ii) that of the upper scanning loop in Figure 5 (the “230” path). Although they both had been started with about the same amount of the molten phase of about 70% and at about the same temperature, their behavior is dramatically different. This can only be explained by different histories of how the initial states had been attained and, therefore, different configurations of the frozen phases. Presumably, upon cooling the system from the completely molten state to the state indicated by “0” in Figure 5, due to strong pore blocking the frozen phase will be composed of the percolating clusters grown from the porous particle boundaries. These clusters may have similar properties with those observed during desorption of fluids from Vycor particles.<sup>25–27</sup> Upon warming to the state “2”, the initially attained configuration undergoes only minor changes (at least this concerns the fraction of the liquid phase which changes only slightly). These minor changes may include, e.g., the elimination of some dead ends. If now the system is cooled down, only those minor changes which have occurred during warming can be restored before the boundary hysteresis is reached. This also explains the return-point memory property, at least for this particular type of scanning loops.

The state with 70% of the molten phase, attained along the warming branch of the boundary hysteresis loop (Figure 3a), may have very different configuration. If melting is predominantly controlled by individual, single-pore properties (which is actually valid for both equilibrium melting or metastable melting via shrinking the solid–liquid interface in radial direction), then melting will occur homogeneously over the pore network. Thus, prior to cooling, the frozen phase is constituted by separated small frozen clusters, occupying neighboring pores with the sufficiently big pore sizes. Upon cooling, these domains will also grow and thus contribute to the freezing process.

### Conclusions

In this work, we have experimentally studied freezing and melting of a fluid in Vycor porous glass by means of NMR cryoporometry. The main objective was to adopt scanning experiments, widely used in adsorption society to study network effects upon sorption of fluids in mesoporous materials, to study

confinement effects upon freezing and melting transitions. As the main conclusion, the scanning freezing and melting behavior is found to be very sensitive to the pore structure of a material under study and the system thermal history. This closely resembles the results obtained for gas sorption in random porous glasses<sup>30</sup> and, therefore, suggests that this approach may become an additional method for structural characterization. It has to be noted that recently this route has also been undertaken, and the potentials of melting and freezing scanning experiments combined with diffusion measurements for assessing the pore-space interconnectivity in polymer microspheres have been demonstrated.<sup>51</sup>

The results obtained allowed to verify earlier findings about the mechanisms of the hysteresis formation as well as to provide some new insight. In particular, they reveal that different cooling and warming histories result in different solid–liquid configurations within the pore system. Such a behavior originates from different pathways relevant for the two transitions. The freezing is found to depend on the existing nuclei of the frozen phase and to be controlled by a strong pore blocking. Therefore, this leads to the formation of percolating continuous clusters of the frozen phase spanning over neighboring pore sections with pore sizes satisfying certain criteria. Melting, on the other hand, is found to be a single-pore property, rendering the transition to occur homogeneously over the whole pore network. Thus, complex cooling and warming cycles may bring about configurations, resulting as an admixture of two different processes. Further evolution of the system from different attained configurations of the solid–liquid phases with changing temperature have been found strongly depend on the system history. Thus, it was shown that starting with the same amount of the frozen phase and roughly from the same temperature, further freezing patterns can be markedly different. Although the origin of such a behavior has been clearly established to result from the different distributions of the frozen phase, details of the space-temporal dependence of freezing are not yet clear. In particular, it would be very interesting to relate the freezing rates for different freezing scanning curves to structural properties of the system under study using percolation theory.

**Acknowledgment.** The authors thank DFG (the German Science Foundation) for the financial support.

(51) Perkins, E. L.; Lowe, J. P.; Edler, K. J.; Rigby, S. P. *Chem. Eng. Sci.* **2010**, *65*, 611–625.